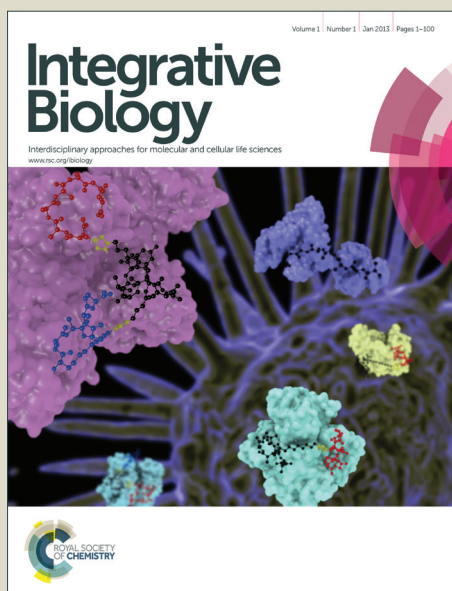


Integrative Biology

Accepted Manuscript



This is an *Accepted Manuscript*, which has been through the Royal Society of Chemistry peer review process and has been accepted for publication.

Accepted Manuscripts are published online shortly after acceptance, before technical editing, formatting and proof reading. Using this free service, authors can make their results available to the community, in citable form, before we publish the edited article. We will replace this *Accepted Manuscript* with the edited and formatted *Advance Article* as soon as it is available.

You can find more information about *Accepted Manuscripts* in the [Information for Authors](#).

Please note that technical editing may introduce minor changes to the text and/or graphics, which may alter content. The journal's standard [Terms & Conditions](#) and the [Ethical guidelines](#) still apply. In no event shall the Royal Society of Chemistry be held responsible for any errors or omissions in this *Accepted Manuscript* or any consequences arising from the use of any information it contains.

Insight, Innovation, Integration:

Lymphatic vessels regulate flow in the tumor microenvironment and secrete factors that attract and facilitate tumor cell invasion, a critical step in metastasis. Their integrated mechanical-biological effects are complex yet important, since interstitial, transmural, and luminal flows can each affect tumor and lymphatic endothelial cells (LECs) to modulate invasion. Here, we develop a robust in vitro model that integrates these flows with image analysis tools to quantitatively assess tumor cell invasion and transmigration across LECs. We demonstrate that MDA-MB-231 tumor cell intravasation is differentially sensitive to interstitial and transmural vs. luminal flows, and when combined, these biomechanical cues additively increase tumor cell invasion. These data provide new mechanistic insight into the mechanobiology of tumor cell invasion into lymphatics.

ARTICLE

An *in vitro* model of the tumor-lymphatic microenvironment with simultaneous transendothelial and luminal flows reveals mechanisms of flow enhanced invasion

Cite this: DOI: 10.1039/x0xx00000x

Received 00th January 2015,
Accepted 00th January 2015

DOI: 10.1039/x0xx00000x

www.rsc.org/

M. Pisano,^a V. Triacca^a, K. A. Barbee^b and M. A. Swartz^{†a,c}

The most common cancers, including breast and skin, disseminate initially through the lymphatic system, yet the mechanisms by which tumor cells home towards, enter and interact with the lymphatic endothelium remain poorly understood. Transmural and luminal flows are important biophysical cues of the lymphatic microenvironment that can affect adhesion molecules, growth factors and chemokine expression as well as matrix remodeling, among others. Although microfluidic models are suitable for *in vitro* reconstruction of highly complex biological systems, the difficult assembly and operation of these systems often only allows a limited throughput. Here we present and characterize a novel flow chamber which recapitulates the lymphatic capillary microenvironment by coupling a standard Boyden chamber setup with a micro-channel and a controlled fluidic environment. The inclusion of luminal and transmural flow renders the model more biologically relevant, combining standard 3D culture techniques with advanced control of mechanical forces that are naturally present within the lymphatic microenvironment. The system can be monitored in real-time, allowing continuous quantification of different parameters of interest, such as cell intravasation and detachment from the endothelium, under varied biomechanical conditions. Moreover, the easy setup permits a medium-high throughput, thereby enabling downstream quantitative analyses. Using this model, we examined the kinetics of tumor cell (MDA-MB-231) invasion and transmigration dynamics across lymphatic endothelium under varying flow conditions. We found that luminal flow indirectly upregulates tumor cell transmigration rate via its effect on lymphatic endothelial cells. Moreover, we showed that the addition of transmural flow further increases intravasation, suggesting that distinct flow-mediated mechanisms regulate tumor cell invasion.

Introduction

An extensive network of lymphatic vessels drain fluid, cells, solutes and antigens from the periphery and, after filtering through the lymph nodes for immune surveillance, deposit their contents in the blood via the thoracic duct. Recent research is increasing our appreciation for the active role that lymphatic endothelium plays in regulating immune and tumor cell transport,¹⁻⁵ and recent studies from our lab and others suggest that lymphatic endothelial cells (LECs) may play important and direct roles in immune tolerance.⁶⁻⁹ However, the mechanisms by which LECs regulate cell transport from the peripheral tissues to the lymph nodes remain unclear. While reports have shown that flow shear stress influences a wide range of blood endothelial cell functions, including leukocyte adhesion and

extravasation,¹⁰⁻¹³ the effects of fluid forces on LEC behaviours – and in particular on its interactions with trafficking leukocytes and tumor cells – has been poorly understood, at least partially due to the lack of biomechanically relevant model systems.

Therefore, the design of an *in vitro* tunable model of the lymphatic microenvironment is a critical step to further explore regulatory mechanisms of the lymphatic network. Such models have the potential to provide useful information about the role of lymphatics in pathological conditions such as cancer or chronic inflammation, and may further support the development of novel and improved therapeutic strategies.

Biomechanically, the lymphatic microenvironment is quite different from that of the blood, and can be characterized by the presence of three types of fluid forces¹⁴: interstitial flow on

interstitial cells, transmural flow on the LECs (basal to apical or abluminal to luminal), and luminal flow parallel to the apical surface of LECs (Fig. 1a-c). Physiologically, we assume that LECs in the absorbing or capillary vessels experience both transmural and luminal flow simultaneously, resulting in a complex pattern of biomechanical cues that may regulate immune or tumor cell motility in addition to interstitial flow (Fig. 1d). Interestingly, it has been observed that the velocity of lymph flow rapidly increases during inflammation and around tumors,^{3,15,16} though the downstream implications of these altered fluid forces on the lymphatic endothelium are not fully understood.

Our group has recently demonstrated that transmural flow modulates dendritic cell and fluid transport across LECs, with higher transmural flow velocities causing LECs to increase their expression of cytokines and adhesion molecules that attract and facilitate leukocyte transmigration such as CCL21, ICAM-1, E-selectin, and VCAM-1.¹⁷ ICAM-1 upregulation by luminal shear stress on LECs has also been suggested to play a role in establishing a pre-metastatic niche in the draining lymph node.¹⁸ Luminal shear stress on LECs can also upregulate endothelial nitric oxide synthase (eNOS), which in turn regulates lymphatic pump function in the collecting vessels.¹⁹⁻²² Finally, luminal shear stress has also been shown to modulate the lymphatic endothelial barrier function by a mechanism dependent upon Rac1-mediated actin dynamics.²³ In these examples, luminal flow was induced across a LEC surface without the ability to recapitulate or observe cell transmigration from the interstitial space into the vessel under relevant flow forces. As such, the role of luminal shear stress on regulating cell transport into lymphatics, as well as its differential effects compared to those of transmural flow, are poorly understood.

As mentioned, conventional *in vitro* experiments do not fully recapitulate the multiple factors that likely contribute strongly to lymphatic function. Migration and transmigration assays have typically been conducted using Boyden chambers²⁴ or parallel plate flow chambers²⁵ for qualitative and quantitative assessment of cellular responses to soluble factors. While these assays are well-established, reliable and easy to setup, they only examine one aspect of the lymphatic microenvironment at a time. In contrast, microfluidic models of the endothelial-interstitial environment have been developed.²⁶⁻³² Microfluidic systems closely match the size dimensions of biological systems, and are thus potentially useful tools for the study of the lymphatic microenvironment. In principle, they allow recapitulation of complex 3D microenvironments and stimulation with precisely defined mechanical forces. However, such setups are typically difficult to use routinely, require skilled expertise, and are less amenable to simultaneously applying different conditions or output parameters. Furthermore, while micro-scale systems allow for direct observation of complex biological processes on the single-cell level, they yield data with small cell numbers, making statistical analyses problematic.

We were interested in developing a 'meso-scale' *in vitro* model that could recapitulate the flow environment of the

lymphatic microenvironment on interstitial cells that enter the lymphatic vessel as well as on the lymphatic endothelium itself, since both of these work in concert during cell trafficking from peripheral tissues such as when tumor cells invade before metastasis (Fig. 1 a-d). To pursue this objective, we designed a culture chamber that allows simultaneous stimulation of LECs with both transmural and luminal flows in a standard cell transmigration assay. Previous work from our group established a simpler model of the tumor-lymphatic microenvironment containing only transmural flow,³⁶ although it was easy to set up and analyze, and amenable to high-throughput experimentation. The new model was designed to keep the simplicity of the earlier model, where the co-cultures could be first established in standard incubator conditions, outside the fluidic device, to ensure LEC confluence and desired morphology before imposing fluid stresses. It was also designed to allow both interstitial and luminal flows to be imposed and controlled individually. We characterized fluid flow patterns in the device, verified cell viability and developed a protocol for high-throughput automated data analyses. Using this new model, we demonstrate how luminal and transmural flows each enhance the invasion and transmigration of MDA-MB-231 tumor cells through the extracellular matrix and across a LEC monolayer.

Materials and Methods

Cell lines

Human dermal LECs were isolated from neonatal foreskin and cultured as described previously.³³ MDA-MB-231 human mammary adenocarcinoma cells were purchased from ATCC and maintained in DMEM with 10% FBS (Gibco, Invitrogen Corp., Carlsbad, CA USA) until 70–80% confluence before being detached and used for the experiments.

Chamber design, fabrication and mounting

To mimic the lymphatic microenvironment (Fig. 1d), the flow chamber was designed to be easy to use and handle, to guaranty cell viability for a time frame of at least 24h, to avoid liquid leakages and to allow time lapse imaging with an inverted fluorescent microscope.

The chamber design was drafted using commercially available CAD software (SolidWorks Corp., Waltham, MA USA). The chamber is composed of three components (Fig. 1f-j): a base, comprising 5 microfluidic channels (500 μm high, 8 mm wide, 40 mm long); a top, which includes the fluidic inlets and outlets, and five regions to house the 6.4 mm cell culture inserts (BD Biosciences, San Jose, CA USA); and caps for each housing, each including a transmural flow inlet. The components were produced by high resolution stereolithography (PROFORM AG, Marly, CH) using U.V. curable resin Somos® Watershed XC11122 (DSM, Heerlen, NL), which is optically transparent and certified to be biocompatible (which we independently verified).

O-rings were placed in the dedicated grooves on the top component and on each cap, in order to seal the microfluidic channels and the cell culture insert, respectively. Before each experiment, the chambers were mounted by placing the top component on the base and tightening with bolts. The devices were then sterilized with ethylene oxide gas for 12h and placed under vacuum for 48h.

Flow control and measurement

Separate peristaltic pumps (IDEX GmbH, Wertheim, DE) were used to generate transmural and luminal flows, which were kept constant throughout the experiments. The transmural flow rate was set at either 0 or 2 $\mu\text{L}/\text{min}$, leading to a transmural flow velocity of 0 or 1 $\mu\text{m}/\text{s}$ across the LEC monolayer. For luminal flow, the flow rates at the luminal inlet were fixed in order to provide the desired shear stress to cells on the membrane (0, 0.01 or 1 dyn/cm^2), according to the Poiseuille approximation for rectangular section channels: $\tau = (6\mu \cdot Q)/(w \cdot h^2)$, where τ is the shear stress (dyn/cm^2), μ is the dynamic viscosity of the culture medium (P), Q is the inlet flow rate (μL), and w and h are the width and the height of the channel, respectively (mm). Starting from this first estimate, a more detailed calculation was done by finite element analyses, as described below. The luminal flow velocity in the channel was also validated with a particle tracking method³⁴ using 5 μm diameter fluorescent beads (Spherotech Inc., Lake Forest, IL), and long exposure times (0.15 s) to calculate their track lengths and thus estimate the average luminal velocity within the channel.

Finite element analysis of the luminal fluid flow distribution

To calculate flow profiles in the chamber, the fluidic channel and the gel compartment were discretized in 3D using COMSOL Multiphysics numerical simulation software (COMSOL Inc., Burlington, MA USA). The geometry of the channel was imported from the original CAD design and a tetrahedral mesh was created. The flow field in the channel was computed using the Navier-Stokes equations, with a fixed inlet flow rate and the outlet pressure set to zero. The above-mentioned equations were coupled with the Darcy equation, accounting for flux in the porous matrix: $\nabla p = -\mu/k \cdot v$, where ∇p is the pressure gradient across the transmural portion, v is the fluid velocity; μ is the fluid viscosity; k is permeability of the 3D matrix, assumed to be 10^{-6} cm^2 as previously determined.³⁵

LEC culture under flow conditions and transmigration assay

LECs were cultured to confluence on the underside (e.g., facing down) of collagen-coated, opaque FluoroblokTM culture inserts (BD Biosciences, San Jose, CA, USA), which contain a 18 μm -thick membrane with pore diameters of 8 μm and which block light transmission from the upper well when visualized from below. Cell tracker green (1 μM , Invitrogen, Carlsbad, CA, USA) was used to label the MDA-MB-231 cells, which were suspended in 1.5 mg/mL type I collagen with 10% Matrigel (both from BD Biosciences) at 10^6 cells/mL and added to the inserts. The matrix was allowed to polymerize for 1h in a humidified incubator at 37°C and 5% CO_2 , during which time

the chamber and tubings were primed with Endothelial Basal medium (EBM with 2% FBS and 0.1% BSA; all from Gibco). In some experiments, 5 $\mu\text{g}/\text{ml}$ mouse anti-human CCR7 neutralizing antibody (MAB197, R&D System, Minneapolis, MN) was added to the medium and to the tumor cell-matrix solution. Following polymerization, the inserts were placed in the flow chamber and sealed with the dedicated caps. Tubing was connected via luer-lock adaptors and fluid flow was introduced at the desired rate.

For transmigration experiments, the chamber was placed on an inverted fluorescence microscope (Axiovert 200 M, Carl Zeiss AG, Feldbach, CH) maintained at 37°C. Images, focused on the LEC monolayer, were acquired every 15 min for 12 h (5 regions per membrane, 5 membranes per experiment). Flowing cell culture medium was saturated in 5% CO_2 and supplemented with HEPES buffer (Gibco).

Cell viability assay

LECs were cultured on the underside of the insert membranes as described above, and subsequently exposed for 24 h under different flow combinations (0, 0.01 or 1 dyn/cm^2 luminal flow and 0 or 1 $\mu\text{m}/\text{s}$ transmural flow) for 24 h. The inserts were then removed from the flow chamber, placed in a standard 24-well plate, rinsed with PBS, and treated with a cell viability assay kit for mammalian cells (Invitrogen) following the manufacturer's protocol. Fluorescence images were acquired and the relative fractions of live vs. dead cells were computed.

Immunostaining

Immunofluorescence staining on the culture inserts was performed with FITC-conjugated mouse anti-human CD31 (1:50, Ancell, Stillwater, MN), mouse anti-human ICAM-1 (1:50, R&D Systems,) and goat anti-human CCL21 (1:25, R&D Systems). Cells were fixed in 2% paraformaldehyde in PBS for 15 min, rinsed with PBS, and immunostained according to standard protocols. Cell nuclei were labelled with 4',6'-diamidino-2-phenylidole (DAPI, Vector Laboratories, Burlingame, CA USA) and imaged using a LSM 700 confocal microscope (Zeiss). Imaris (Bitplane AG, Zurich, CH) was used for the z-stack reconstruction.

Quantification of cell transmigration

During the imaging acquisition process, the focal plane was maintained on the luminal side of the LEC monolayer. Due to the light-blocking insert membranes, fluorescence from the labeled tumor cells could only be detected from the luminal side. We could ensure that the fluorescent objects that we tracked represented transmigrated tumor cells (rather than, for example, abuminally positioned cells that might, extend cell projections across the LECs) by their size and by tracking in the x-y plane their movements across the LEC surface until they detached and disappeared from the focal plane.

The images acquired during the transmigration experiments were processed with ImageJ (NIH, Bethesda, MD USA) using a custom macro to identify the cells. Imaris (Bitplane AG, Zurich, CH) was used with its tracking algorithm to

automatically extrapolate the appearance, trajectory, and disappearance of each tumor cell from the membrane. An in-house Matlab (Mathworks, Natick, MA) code was used to obtain the transmigration dynamics, transmigration rates and adhesion times of each cell.

Results and Discussion

Characterization of luminal flow in the chamber

To characterize the flows induced on the LECs cultured on the insert membranes, we measured flow velocities in the channel for each fixed inlet flow rate using fluorescent beads and time lapse fluorescent imaging as previously described.³⁴ The measured average velocities were consistent with Poiseuille flow profiles (Fig. 2a), confirming the correct positioning of the insert membrane at 500 μm from the chamber bottom. The computationally estimated shear stress profiles on the luminal surface of the LECs (Fig. 2c) further demonstrated that when both transmural and luminal flows were present, the contribution from transmural flow to the overall average luminal shear stress was negligible (Fig. 2b). Even with the lowest average luminal flow rate used, the transmural flow increased the average luminal shear stress by roughly 5%, and the maximum shear stress (i.e., at the downstream end of the membrane, relative to the luminal flow direction) by $\sim 20\%$.

LECs form and maintain a viable monolayer under different flow conditions

The integrity of the LEC monolayer after 24 h culture in the device was confirmed by fluorescence microscopy. The LECs remained confluent and viable, with no visible differences in expression patterns of cell-cell junctions (PECAM-1, Fig. 3a) or in cell viability (Fig 3b,c) between static and flow conditions. Of course, many features of the *in vivo* lymphatic vessel cannot be recapitulated in this *in vitro* system, and it is unknown how the more complex microenvironment around a lymphatic vessels affects cell transmigration; however, the system allows us to carefully control the biomechanical environment and monitor subtle changes in cell migration, which would be difficult to achieve *in vivo*.

Quantification of cell transmigration dynamics

In our previous work,³⁶ we assessed transmigrated tumor cells at a single time point and could not differentiate between cells that had transmigrated early on (i.e., those that were positioned near the abluminal side of the LECs at the start) from those that had transmigrated later (i.e., those that also had to invade through the ECM). Furthermore, because transmigrated tumor cells could either stay attached to the LEC monolayer, detach and float, or settle and attach to the plastic bottom of the well, three compartments had to be analyzed for each sample: the

apical side of the LEC monolayer, the bottom of the culture dish, and the medium in between. To avoid these issues and also record the kinetics of each transmigrated cell, we performed live imaging on multiple regions of the apical side of each sample over 6 h.

We used opaque insert membranes and imaged from the focal plane fixed on the LEC luminal surface so that fully transmigrated, fluorescently labelled tumor cells could be clearly distinguished by their size and their movement along the x-y plane. Representative confocal images in the z-plane confirmed that LECs remained confluent and firmly adhered to the membrane and that transmigrating tumor cells were only seen on the luminal, not the abluminal, surface of the LECs (Supplementary Fig S1).

We developed an algorithm to identify and track the trajectories of each cell appearing on the membrane over time (Fig. 4a, b), since we found that simply counting the number of transmigrated cells present on the membrane at each timepoint was not accurate in reflecting the true transmigration rate due to the inability to account for those cells that have detached in the meantime (Fig. 4c, d). By tracking each cell individually and recording when it both appears and disappears from the luminal surface, we can obtain a more accurate picture of the transmigration dynamics.

Luminal and transmural flows increase MDA-MB-231 transmigration rate and modulate their adhesion to the lymphatic endothelium

Cell intravasation in the lymphatic capillaries is a critical step in tumor cell dissemination and metastasis. Most carcinomas sprout from the primary tumor into the surrounding interstitial space, invade the surrounding tissues, and eventually intravasate into lymphatic vessels to disseminate.³⁷ To explore the effects of various fluid forces on tumor cell transmigration, we used our new model to examine first the role of luminal shear flow. Based on previous estimations, the velocity of the lymph in the lymphatic capillaries in a mouse tail model is in the range of 5-30 $\mu\text{m/s}$,³⁸ leading to wall shear stresses between 0.01-0.06 dyn/cm^2 . In a rat mesenteric pre-nodal lymphatic model, the intraluminal flow has been shown to lead to an average shear stress of about 0.6 dyn/cm^2 , with peaks of 4-12 dyn/cm^2 .³⁹ Lymph flow in the lymphatic capillaries is highly variable, depending on the location in the body. Moreover, it is increased during inflammatory events.^{17,40} Fisher and collaborators measured resting average lymph flow velocities in human skin lymphatic capillaries and found values in the range of 7-14 $\mu\text{m/s}$.⁴¹ Assuming a viscosity of 1.5 cP ⁴² and a Hagen-Poiseuille flow, the relative shear stress would be between 0.01 and 0.04 dyn/cm^2 .

Based on these data, we decided to examine the effect of two different shear stress values, 0.01 (low shear) and 1 (high shear) dyn/cm^2 , modeling the shear forces present in the lymphatic capillaries during physiological conditions and inflammation, respectively.

Interestingly, we observed a shear flow dependent increase in MDA-MB-231 breast cancer cell transmigration rate across the lymphatic wall (Fig. 5a, b).

These data show for the first time that luminal shear stress indirectly affects tumor cells in the interstitial space through its action on the lymphatic endothelium, which in turn actively modifies the surrounding microenvironment and modulates tumor cell migration dynamics.

Moreover, we examined MDA-MB-231 adhesion time on the endothelial monolayer after transmigration, but we couldn't observe any significant effect of luminal flow (Fig. 5c).

We then investigated whether the combination of luminal and transmural flow has an effect on tumor cell transmigration. Indeed, simultaneous shear stress and transmural mechanical stimuli provoked an upregulation of intravasation higher than when the single flows were applied (Fig. 5d), as indicated by a significant increase in the transmigration rate (Fig. 5e).

It is important to note that transmural flow alone, set at a velocity of $1\mu\text{m/s}$, caused a significant increase of cell transmigration (Fig. 5e). These findings are consistent with what has been previously reported using the standard transwell system.⁴³ Nevertheless, combining transmural and luminal flows doubled the number of transmigrated cells with respect to luminal flow alone (Fig. 5d). In addition, we observed that transmural flow promotes cell adhesion to the endothelium when compared to luminal flow, suggesting that these distinct biomechanical cues have opposite effects in modulating cell adhesion to lymphatics (Fig. 5f). Interestingly, when we combined the two stimuli we noticed a significant increase in the adhesion time of the tumor cells on the endothelium, as there are significantly less cells detaching after less than 1 hour of adhesion respect to the static condition and significantly more cells still adherent after 3 hours respect to the luminal flow condition (Fig. 5f).

These results show that our *in vitro* model is capable of detecting differences in tumor cell transmigration across a lymphatic monolayer in response to different biophysical stimuli. Previous studies had shown and justified the effect of transmural flow on tumor cell intravasation *in vitro*, but the effect of luminal or luminal plus transmural flows could not be investigated because of the lack of reliable model systems. Here, we have confirmed previously published data obtained with well-established systems, and we have given evidences for a new mechanism of regulation of tumor cell migration, not observable with any other existing system.

The flow-mediated change in tumor cell transmigration observed here could be attributed to multiple factors. We previously demonstrated that transmural flow strongly induces CCL21 expression by LECs,¹⁷ which engages with ICAM-1 to facilitate cell transmigration. Here, we found that luminal shear stress also induces CCL21 upregulation by LECs (Fig. 6a, b). Flow-enhanced CCL21 upregulation was required for the flow-enhanced tumor cell transmigration, since blocking antibodies against CCR7 signaling prevented this effect (Fig. 6c).

CCL21 is known to strongly bind extracellular matrix proteoglycans, and we previously measured its binding constant

K_D ($k_{\text{off}}/k_{\text{on}}$) to the Matrigel-collagen matrix used here as $K_D=7\text{nM}$.⁴³ This strong binding should counteract convection-driven forces into the lymphatic lumen. Such low binding constant allows the chemokine not to be transported away from the endothelium by the convective flows. To further confirm this, we perform a z-stack confocal imaging of an exogenous CCL21 gradient in a Matrigel-collagen matrix, both in static and flow condition, revealing no difference between the two (Supplementary Fig. S2).

Moreover, the effect of an overexpression of a non-matrix-binding chemokine by the lymphatic endothelium would also affect the tumor cell in the extracellular space, since the Peclet number in our system is in the order of 0.1, indicating that diffusion dominates over convection in the matrix (although the effect of convection cannot be ignored).

Interstitial flow on tumor cells has been shown to cause counterbalanced directional clues upstream (CCR7 independent) or downstream (CCR7 dependent) with respect to interstitial flow; this balance was found to be dependent on the cell density in the matrix.⁴⁴ In particular, our group has recently demonstrated that it is possible to identify distinct tumor subpopulations, one of which responds with a high directedness towards the flow stream.⁴³

While interstitial flow effect on tumor cell migration has been already examined, here we show for the first time that luminal flow is a potential regulator of the lymphatic function through its action on CCL21 expression. To further investigate this hypothesis, we performed the transmigration experiments with different level of luminal flow, in presence or absence of a CCR7 blocking antibody (Fig. 6c). We observed that blocking CCR7 signalling abolished luminal flow – driven transmigration of MDA-MB-231 cells, thus confirming that luminal flow can drive CCR7-expressing tumor cell transmigration across a lymphatic endothelium through the regulation of CCL21 in LECs.

However, luminal and transmural flow may have a much broader impact on lymphatic function, and further studies are needed to clarify new regulation pathways dependent on such biomechanical stimuli.

Conclusions

We have presented and characterized a novel flow chamber, which combines a standard Boyden chamber assay with controlled microfluidics to simulate *in-vivo*-like biomechanics. Indeed, we were able to model the different compartments of the microenvironment of a lymphatic capillary (vessel lumen, vessel wall and extracellular space) and its specific biomechanical cues (transmural and luminal flow). Moreover, the presented system allows for the study of cell transmigration across a LEC monolayer; it permits the quantification of cell transmigration dynamics, transmigration rates and cell detachment from the endothelium.

Our platform was applied to study the role of transmural and luminal flow on intravasation of a breast cancer cell line

(MDA-MB-231) across a LEC monolayer. We demonstrated that luminal flow indirectly increases tumor cell transmigration by its action on LECs, specifically by upregulating CCL21 expression. We have also demonstrated that luminal and transmural flow increase tumor cell transmigration more than luminal flow alone. Our study provides new insights regarding flow-mediated regulation of tumor migration in the lymphatic system, and presents a novel in vitro tool for further research on potential targets for cancer therapy.

Acknowledgements

The authors are grateful to Samuel Gex, Olivier Burri, and Cara Buchanan for helpful advice and assistance. This study was funded by grants from the Swiss National Science Foundation (31-135756) and the European Research Commission (AdG – 323053).

Notes and references

^aInstitute of Bioengineering and Swiss Institute for Experimental Cancer Research (ISREC), School of Life Sciences, École Polytechnique Fédérale de Lausanne (EPFL), Lausanne, Switzerland.

^bSchool of Biomedical Engineering, Science, and Health Systems; Drexel University, Philadelphia, PA, USA.

^cInstitute for Molecular Engineering, University of Chicago, Chicago, IL, USA.

†Corresponding author. Email: melodyswartz@uchicago.edu.

- M. L. Kahn and D. J. Rader, *Cell Metab*, 2013, **17**, 627-628.
- G. J. Randolph, V. Angeli and M. A. Swartz, *Nat Rev Immunol*, 2005, **5**, 617-628.
- H. Wiig and M. A. Swartz, *Physiol Rev*, 2012, **92**, 1005-1060.
- J. D. McAllaster and M. S. Cohen, *Adv Drug Deliv Rev*, 2011, **63**, 867-875.
- A. Gogineni, M. Caunt, A. Crow, C. V. Lee, G. Fuh, N. van Bruggen, W. L. Ye and R. M. Weimer, *Plos One*, 2013, **8**.
- F. V. D. A. W. Lund, S. Hirose, V. R. Raghavan, C. Nembrini, S. N. Thomas, A. Issa, S. Hugues, M. A. Swartz, *Cell Rep*, 2012, **1**, 1-9.
- E. F. Tewalt, J. N. Cohen, S. J. Rouhani, C. J. Guidi, H. Qiao, S. P. Fahl, M. R. Conaway, T. P. Bender, K. S. Tung, A. T. Vella, A. J. Adler, L. Chen and V. H. Engelhard, *Blood*, 2012, **120**, 4772-4782.
- M. A. Swartz and A. W. Lund, *Nat Rev Cancer*, 2012, **12**, 210-219.
- S. Hirose, E. Vokali, V. R. Raghavan, M. Rincon-Restrepo, A. W. Lund, P. Corthesy-Henrioud, F. Capotosti, C. Halin Winter, S. Hugues and M. A. Swartz, *J Immunol*, 2014, **192**, 5002-5011.
- N. Resnick, H. Yahav, A. Shay-Salit, M. Shushy, S. Schubert, L. C. Zilberman and E. Wofovitz, *Prog. Biophys. Mol Biol*, 2003, **81**, 177-199.
- B. D. Johnson, K. J. Mather and J. P. Wallace, *Vasc Med*, 2011, **16**, 365-377.
- K. Yamamoto and J. Ando, *J Pharmacol Sci*, 2011, **116**, 323-331.
- S. Liang, M. J. Slattery, D. Wagner, S. I. Simon and C. Dong, *Ann Biomed Eng*, 2008, **36**, 661-671.
- M. A. Swartz, *Adv Drug Deliv Rev*, 2001, **50**, 3-20.
- A. M. Tchafa, A. D. Shah, S. Wang, M. T. Duong and A. C. Shieh, *J Vis Exp*, 2012, **65**, 4159.
- P. Koumoutsakos, I. Pivkin and F. Milde, *Annu Rev Fluid Mech*, 2013, **45**, 325-355.
- D. O. Miteva, J. M. Rutkowski, J. B. Dixon, W. Kilariski, J. D. Shields and M. A. Swartz, *Circ Res*, 2010, **106**, 920-931.
- Y. Kawai, M. Kaidoh, Y. Yokoyama and T. Ohhashi, *Cancer Sci*, 2012, **103**, 1245-1252.
- Y. Kawai, Y. Yokoyama, M. Kaidoh and T. Ohhashi, *Am J Physiol Cell Physiol*, 2010, **298**, C647-C655.
- H. G. Bohlen, O. Y. Gasheva and D. C. Zawieja, *Am J Physiol: Heart Circ Physiol*, 2011, 301, H1897-H1906.
- G. W. Schmid-Schonbein, *Proc Natl Acad Sci USA*, 2012, **109**, 3-4.
- A. M. Andrews, D. Jaron, D. G. Buerk, P. L. Kirby and K. A. Barbee, *Nitric Oxide*, 2010, **23**, 335-342.
- J. W. Breslin and K. M. Kurtz, *Lymphat Res Biol*, 2009, **7**, 229-237.
- Z. Pujic, D. Mortimer, J. Feldner and G. J. Goodhill, *Comb Chem High Throughput Screen*, 2009, **12**, 580-588.
- S. A. Parsons, C. Jurzinsky, S. L. Cuvelier and K. D. Patel, *Methods Mol Biol*, 2013, **946**, 285-300.
- S. Chung, R. Sudo, P. J. Mack, C. R. Wan, V. Vickerman and R. D. Kamm, *Lab Chip*, 2009, **9**, 269-275.
- M. K. Shin, S. K. Kim and H. Jung, *Lab Chip*, 2011, **22**, 3880-3887.
- J. S. Jeon, I. K. Zervantonakis, S. Chung, R. D. Kamm and J. L. Charest, *Plos One*, 2013, **8**.
- K. H. Wong, J. M. Chan, R. D. Kamm and J. Tien, *Annu Rev Biomed Eng*, 2012, **14**, 205-230.
- E. Bianchi, R. Molteni, R. Pardi and G. Dubini, *J Biomech*, 2013, **46**, 276-283.
- C. Buchanan and M. N. Rylander, *Biotechnol Bioeng*, 2013, **110**, 2063-2072.
- M. B. Chen, J. A. Whisler, J. S. Jeon and R. D. Kamm, *Integr Biol*, 2013, **5**, 1262-1271.
- S. Podgrabinska, P. Braun, P. Velasco, B. Kloos, M. S. Pepper and M. Skobe, *Proc Natl Acad Sci USA*, 2002, **99**, 16069-16074.
- C. K. Tung, O. Krupa, E. Apaydin, J. J. Liou, A. Diaz-Santana, B. J. Kim and M. Wu, *Lab Chip*, 2013, **13**, 3876-3885.
- C. P. Ng and M. A. Swartz, *Am J Physiol: Heart Circ Physiol*, 2003, **284**, H1771-1777.
- J. D. Shields, M. E. Fleury, C. Yong, A. A. Tomei, G. J. Randolph and M. A. Swartz, *Cancer Cell*, 2007, **11**, 526-538.
- J. P. Sleeman and W. Thiele, *Int J Cancer*, 2009, **125**, 2747-2756.
- D. A. Berk, M. A. Swartz, A. J. Leu and R. K. Jain, *Am J Physiol*, 1996, **270**, H330-H337.
- J. B. Dixon, S. T. Greiner, A. A. Gashev, G. L. Cote, J. E. Moore and D. C. Zawieja, *Microcirculation*, 2006, **13**, 597-610.
- Z. Yuan, H. Rodela, J. B. Hay, D. Oreopoulos and M. G. Johnston, *Lymphology*, 1994, **27**, 114-128.
- M. Fischer, U. K. Franzeck, I. Herrig, U. Costanzo, S. Wen, M. Schiesser, U. Hoffmann and A. Bollinger, *Am J Physiol*, 1996, **270**, H358-H363.
- V. T. Turitto, *Prog Hemost Thromb*, 1982, **6**, 139-177.
- U. Haessler, J. C. Teo, D. Foretay, P. Renaud and M. A. Swartz, *Integr Biol*, 2012, **4**, 401-409.
- W. J. Polacheck, J. L. Charest and R. D. Kamm, *Proc Natl Acad Sci USA*, 2011, **108**, 11115-11120.

45. S. Sheikh, G. E. Rainger, Z. Gale, M. Rahman and G. B. Nash, *Blood*, 2003, **102**, 2828-2834.
46. J. J. Chiu, L. J. Chen, P. L. Lee, C. I. Lee, L. W. Lo, S. Usami and S. Chien, *Blood*, 2003, **101**, 2667-2674.